



# Reactivity of performic acid with organic and inorganic compounds: from oxidation kinetic to reaction pathways

Christelle Nabintu Kajoka, Johnny Gasperi, S. Brosillon, Emilie Caupos, Emmanuelle Mebold, Marcos Oliveira, Vincent Rocher, Ghassan Chebbo, Julien Le Roux

## ► To cite this version:

Christelle Nabintu Kajoka, Johnny Gasperi, S. Brosillon, Emilie Caupos, Emmanuelle Mebold, et al.. Reactivity of performic acid with organic and inorganic compounds: from oxidation kinetic to reaction pathways. ACS ES&T Water, 2023, 3 (9), pp.3121-3131. 10.1021/acsestwater.3c00279 . hal-04195028

**HAL Id: hal-04195028**

**<https://enpc.hal.science/hal-04195028>**

Submitted on 4 Sep 2023

**HAL** is a multi-disciplinary open access archive for the deposit and dissemination of scientific research documents, whether they are published or not. The documents may come from teaching and research institutions in France or abroad, or from public or private research centers.

L'archive ouverte pluridisciplinaire **HAL**, est destinée au dépôt et à la diffusion de documents scientifiques de niveau recherche, publiés ou non, émanant des établissements d'enseignement et de recherche français ou étrangers, des laboratoires publics ou privés.

# Reactivity of performic acid with organic and inorganic compounds: from oxidation kinetic to reaction pathways

*Christelle Nabintu Kajoka<sup>1</sup>, Johnny Gasperi<sup>2</sup>, Stephan Brosillon<sup>3</sup>, Emilie Caupos<sup>1</sup>, Emmanuelle Mebold<sup>5</sup>, Marcos Oliveira<sup>4</sup>, Vincent Rocher<sup>4</sup>, Ghassan Chebbo<sup>1</sup>, Julien Le Roux<sup>1,\*</sup>*

<sup>1</sup> LEESU, Ecole des Ponts, Univ Paris Est Creteil, F-94010 Creteil, France

<sup>2</sup> LEE - Laboratoire Eau et Environnement, Université Gustave Eiffel, F-44344 Bouguenais, France

<sup>3</sup> IEM - Institut Européen des Membranes, Université de Montpellier, F-34090 Montpellier, France

<sup>4</sup> SIAAP - Service Public de l'assainissement Francilien (SIAAP), Direction Innovation, F-92700 Colombes, France

<sup>5</sup> Observatoire des Sciences de l'Univers OSU-EFLUVE, plateforme PRAMMICS, Université Paris Est Créteil, CNRS, F-94010, Créteil, France

\*Corresponding author: Tel.: +33(0)182392080; e-mail: [julien.le-roux@u-pec.fr](mailto:julien.le-roux@u-pec.fr)

## KEYWORDS

organic peracid, micropollutants, kinetic rate constants, wastewater, oxidation byproducts

## SYNOPSIS

This work describes the kinetics of performic acid autodecomposition and oxidation of organic compounds, and the most reactive functional groups leading to oxidation byproducts.

## ABSTRACT

Performic acid (PFA) has gained interest as an alternative chemical disinfectant for wastewater (WW) treatment, but its reactivity with WW constituents remains poorly understood. This study evaluated PFA's ability to oxidize 45 inorganic and organic compounds commonly found in WW (amino acids, simple organic compounds with specific functional groups, e.g., amines and phenolic compounds, and pharmaceutical micropollutants). PFA does not react with most major ions, except for iodide ion, and reacts with iron(II) in the absence of phosphate buffer. While many organic molecules do not react with PFA, compounds containing reduced-sulfur moieties (e.g., thioether or thiol) are the most reactive (i.e., ranitidine, benzenethiol and 3-mercaptophenol), followed by compounds with tertiary amine groups (e.g., lidocaine). The reactions follow second-order kinetics with respect to both organic compounds and PFA concentrations. Similar trends were observed in real WW effluents, although removals of pharmaceuticals were lower than expected due to the probable consumption of PFA by WW constituents (dissolved organic carbon, other micropollutants, or transition metals). The results highlight PFA's selective reactivity with specific functional groups, and a low transformation of compounds mostly through oxygen addition (e.g., S-oxide or sulfonyl compounds formed from thiol and thioether moieties and N-oxides from amine groups) with similar mechanisms to peracetic acid.

## 1. INTRODUCTION

Among organic peracids, performic and peracetic acids (PFA and PAA, respectively) have recently emerged in wastewater (WW) treatment as alternative disinfectants because of their efficiency against a wide range of microorganisms<sup>1–3</sup> and because they are easy to implement technically.<sup>4</sup> The effectiveness of PFA has been demonstrated for disinfecting primary,<sup>2</sup> secondary,<sup>5,6</sup> and tertiary<sup>7</sup> WW, as well as combined sewer overflow (CSO) reservoirs,<sup>8,9</sup> with faster disinfection kinetics than PAA and/or chlorine.<sup>5,10</sup> Furthermore, peracids form very few disinfection byproducts (DBPs) compared to traditional disinfectants such as chlorine or ozone.<sup>3,7,11</sup> Under typical water treatment conditions (oxidant < 10 mg/L), the formation of halogenated DBPs and N-nitrosamines by PFA and/or PAA is negligible.<sup>6,12</sup> In addition, the use of PFA has been associated with the absence of toxicological effects in disinfected secondary WW.<sup>13,14</sup>

Due to its instability, PFA is not commercially available as a ready-to-use chemical solution and must be produced on-site through the reaction ((1) between hydrogen peroxide (H<sub>2</sub>O<sub>2</sub>) and formic acid (FA), which can be acid-catalyzed by a strong acid, typically sulfuric acid.<sup>15</sup> As the reaction is reversible, the resulting solution is a quaternary equilibrium mixture always containing FA, water, and two oxidants, PFA and H<sub>2</sub>O<sub>2</sub>. At the industrial scale, Kemira Oyj has developed a PFA production system that has already been implemented in Italy, Germany, and France.<sup>5,16</sup>



In addition to its disinfectant properties, the oxidation potential of PFA (1.537 V/Standard Hydrogen Electrode, SHE) is higher than those of H<sub>2</sub>O<sub>2</sub> (1.349 V/SHE), PAA (1.361 V/SHE), and chlorine (1.288 V/SHE), but lower than that of ozone (1.720 V/SHE).<sup>17</sup> Despite the growing use of PFA, little attention has been paid to its ability to react with the organic and inorganic

compounds commonly present in WW. A poor removal (<8%) of 8 pharmaceutical micropollutants was previously reported from primary-treated WW (dissolved organic carbon = 90–110 mg/L) with a PFA dose of 6 mg/L.<sup>18</sup> Bisphenol-A was not degraded by PFA in deionized water and within 1 hour of reaction.<sup>7</sup> Ragazzo et al.<sup>5</sup> also found that PFA had poor oxidation power toward phenols (at PFA doses of 0.7–1.4 mg/L for 14–30 min) or hormones such as estrone (at doses of 2–20 mg/L for 30 min). As PAA and PFA have been identified as weak oxidants for the removal of organic micropollutants, they require activation in order to become effective oxidizers. The activation of PAA has already been tested using transition metals ( $\text{Cu}^{2+}$ ,  $\text{Co}^{2+}$ ,  $\text{Fe}^{2+}$ , and  $\text{Mn}^{2+}$ ) or UV irradiation,<sup>19,20</sup> which has been proven to enhance the degradation of organic compounds.

This study aimed to acquire a deeper understanding of the reactivity of PFA and its oxidation potential toward substances containing various chemical functional groups. Specifically, the study aimed to: 1) investigate the reactivity of PFA in pure solutions by examining its consumption by various organic and inorganic compounds potentially present in WW; 2) determine the kinetic rate constants of decomposition of some simple organic compounds and pharmaceutical compounds by PFA; 3) evaluate some factors that influence the reaction kinetics (e.g., WW matrix, pH); and 4) identify some transformation products and elucidate the reaction pathways. To the best of our knowledge, this is the first study to address these objectives.

## 2. MATERIALS AND METHODS

### 2.1. Chemical Reagents

All the solvents and chemicals were used as received without further purification. Details regarding chemicals (purity and suppliers) are provided in Text S1 (Supporting Information,

SI). The solutions of organic compounds were prepared in methanol, and working solutions were obtained by dilution in deionized (DI) water (Milli-Q, 18 MΩ·cm).

## 2.2. PFA Preparation and Measurement

PFA was prepared using a method developed by Kemira (KemConnect DEX) and adapted by Nihemaiti et al.,<sup>21</sup> consisting of two steps (31.20 mL of 99% formic acid mixed with 0.15 mL of cold water and 2.65 mL of 98% sulfuric acid and 5.43 mL of this mixture reacted with 6.89 mL of 50% H<sub>2</sub>O<sub>2</sub> for 90 min in an ice bath). The resulting PFA stock solution contained approximately 19.5 ± 1.4% (233.9 ± 16.6 g/L) and 19.2 ± 1.2% (230.4 ± 13.8 mg/L) by weight of H<sub>2</sub>O<sub>2</sub> and PFA, respectively.

The quantification of high concentrations (>10 mg/L) of PFA and H<sub>2</sub>O<sub>2</sub> was performed using the iodometric method, as reported by Rocher & Azimi (Text S2, SI).<sup>6</sup> For PFA concentrations <10 mg/L, the measurement was performed with the DPD colorimetric method developed by Dominguez et al.<sup>22</sup> for PAA and adapted here for PFA (Text S2, Figure S1, SI).

## 2.3. Autodecomposition Kinetics of Peracids

The autodecomposition rates of PFA and PAA were determined either in DI water or in 10 mM phosphate buffer solution (PBS) at different pHs (from 2.3 to 11.0). After PFA titration by the iodometric method, the required volume of peracid was injected into 200 mL of PBS or DI water in a beaker to achieve a peracid initial concentration of 1.8 ± 0.3 mg/L for PFA and 0.4 or 0.8 mg/L for PAA (respectively for pH 5.9 and 7.7). Samples were periodically taken to measure the residual peracid concentration by the DPD colorimetric method. All experiments were conducted at least in duplicate. Kinetic modeling was performed using COPASI.<sup>23</sup>

The autodecomposition of peracids followed first-order kinetics (eq 2).

$$\frac{d [\text{peracid}]}{dt} = - k_{\text{peracid}} \times [\text{peracid}] \quad (2)$$

111 Where  $k_{\text{peracid}}$  is the observed first-order rate constant for PFA or PAA and  $[\text{peracid}]$  is the  
112 concentration of PFA or PAA (mg/L).

113 The linearization of eq 2 (eq 3) showed a good fit with experimental values, confirming the  
114 first-order kinetics, and kinetic rate constants were derived from the slope of 3 and are expressed  
115 in  $\text{min}^{-1}$ .

$$\ln \left( \frac{[\text{peracid}]}{[\text{peracid}]_0} \right) = - k_{\text{peracid}} \times t \quad (3)$$

116 Where  $[\text{peracid}]_0$  is the initial concentration of PFA or PAA (mg/L).

#### 117 2.4. Reactivity of PFA with Inorganic and Organic Compounds

118 The reactivity of PFA was studied by examining its consumption by 45 compounds: 7 inorganic  
119 compounds (ammonia nitrogen, nitrite, bromide, iodide, chloride, iron(II), and hydrogen  
120 phosphate ions), 8 amino acids (glycine, methionine, cysteine, histidine, glutamine, tyrosine,  
121 tryptophan, and asparagine), 1 derived amino acid (taurine), 14 simple model organic  
122 compounds [morpholine, aniline, dimethylamine (DMA), trimethylamine (TMA), urea, furan,  
123 thiophene, resorcinol, phenol, hydroquinone, catechol, benzenethiol, 3-mercaptophenol and 4-  
124 aminophenol], and 15 pharmaceutical compounds (diclofenac, acetaminophen, lidocaine,  
125 naproxen, 17 $\alpha$ -ethinylestradiol, carbamazepine, sulfadiazine, sulfamethoxazole, ciprofloxacin,  
126 bisphenol A, tramadol, trimethoprim, ranitidine, furosemide and amoxicillin).

127 The 7 inorganic compounds were selected because they are typically present in WW, and some  
128 are known to interact with various oxidants, such as ozone,<sup>24</sup> chlorine,<sup>25,26</sup> and PAA.<sup>27</sup>  
129 Regarding organic compounds, it was important to first understand the degradation mechanisms  
130 of simple functional groups (using model organic compounds) before studying the reactivity of  
131 pharmaceuticals that typically contain multiple functional groups. The selection of  
132 pharmaceuticals was based on their frequent detection in Parisian WW,<sup>28</sup> while amino acids

were studied due to their common occurrence in WW as constituents of organic matter. Two sets of experiments were conducted: one in PBS (10 mM, pH 7.0) for all compounds and another in DI water (with the initial pH adjusted at 7.1 with NaOH before PFA addition) for iron(II) only. In all experiments, the solutions of the investigated compounds were prepared at 8  $\mu$ M, and 16  $\mu$ M of PFA was added under stirring to initiate the reaction. After 10 min of reaction, aliquots of the solution were collected to measure the PFA consumption by each compound. All experiments were performed at least in triplicates and at  $20.0 \pm 1.0$  °C. The PFA consumption was normalized by dividing the residual concentrations of PFA in the solution containing the compound by the concentration in the solution of PFA alone (PFA control obtained by autodecomposition), resulting in the residual concentration ratio (RCR).

## 2.5. Decomposition Kinetics of Model and Pharmaceutical Compounds

All decomposition kinetic rate constants were determined in 100 mL of PBS (10 mM, pH 7.0) containing 1  $\mu$ M of each molecule of interest. The working solution was placed under stirring in a thermostatic chamber at  $20.0 \pm 1.0$  °C (in an amber bottle and protected from light), and PFA was added to initiate the reaction ( $[PFA]_0 = 500$   $\mu$ M). In order to be in pseudo-first-order and facilitate the calculation of kinetic rate constants, the initial concentration of the oxidant was 500 (PFA) or  $\sim 900$  times ( $H_2O_2$ ) that of the molecule. Under these conditions,  $\sim 30\%$  of the initial PFA concentration remained at the end of the reaction ( $\sim 150$   $\mu$ M), which indicates that PFA was still in excess compared to the organic compound. At fixed time intervals, 1.5 mL of the sample was transferred to an amber vial containing 50  $\mu$ L of 0.1 M  $Na_2S_2O_3$  ( $[Na_2S_2O_3]_0/[PFA]_0 = 7$ ) to stop the reaction before analysis (Section 2.7). Since  $H_2O_2$  (892  $\mu$ M,  $30.34 \pm 0.75$  mg/L) is always present in the PFA working solution (500  $\mu$ M, 31 mg/L), control experiments were conducted using pure  $H_2O_2$  at the same concentration as that present in the PFA solution in order to evaluate its contribution to decomposition kinetics. All kinetic



experiments were performed in triplicates with a maximum reaction time of 30 min. Sample vials were kept at 4 °C prior to analysis.

For all model and pharmaceutical compounds, the plots of  $\ln([\text{organic compound}]/[\text{organic compound}]_0)$  versus time showed good linearity, suggesting that the reaction was pseudo-first-order with respect to the organic compound, and the observed rate constant,  $k_{\text{obs}}$  ( $\text{min}^{-1}$ ), was derived from the slope. The decomposition of the model and pharmaceutical compounds by PFA can thus be described as second-order kinetics (eq 4), and the kinetic rate constants,  $k_{\text{app}}$  ( $\text{M}^{-1} \text{s}^{-1}$ ), were calculated by dividing  $k_{\text{obs}}$  by the initial concentration of PFA.

$$\begin{aligned} \frac{d [\text{organic compound}]}{dt} &= - k_{\text{obs}} \times [\text{organic compound}] \\ &= - k_{\text{app}} \times [\text{PFA}] \times [\text{organic compound}] \end{aligned} \quad (4)$$

where  $k_{\text{obs}}$  ( $\text{min}^{-1}$ ) is the observed kinetic rate constant for the pseudo-first-order and  $k_{\text{app}}$  ( $\text{M}^{-1} \text{s}^{-1}$ ) is the second-order rate constant for the organic compound; [PFA] and [organic compound] are the concentrations of PFA and the organic compound, respectively.

## 2.6. Reactions in Wastewater Effluent

Treated WW effluent was collected from the Seine Amont WWTP located in Valenton, France, as previously described.<sup>21</sup> Samples were collected directly before the discharge channel and were filtered upon arrival in the laboratory through a 0.7  $\mu\text{m}$  glass fiber filter (Whatman). The WW quality parameters were as follows (mean  $\pm$  standard deviation (SD) over three samples): pH  $7.9 \pm 0.1$ , total suspended solids  $5.5 \pm 2.8$  mg/L, UV254  $1.1 \pm 0.6$ , nitrite  $0.55 \pm 0.12$  mg/L as N, ammonium  $1.56 \pm 1.00$  mg/L as N, phosphate  $3.08 \pm 0.93$  mg/L as P, dissolved organic carbon  $8.06 \pm 0.73$  mg/L, and temperature  $22.9 \pm 0.6$  °C.

Batch oxidation experiments were conducted on the actual WW effluent without pH adjustment. The effluent was spiked with 7 pharmaceutical compounds at 1  $\mu\text{g/L}$  ( $\sim 4 \times 10^{-3}$   $\mu\text{M}$ )

each: ranitidine (RAN), lidocaine (LID), furosemide (FUR), diclofenac (DCF), acetaminophen (ACT), sulfamethoxazole (SMX), and carbamazepine (CBZ). The analysis of the non-spiked WW sample revealed the presence of these pharmaceuticals at various concentrations ( $C_0$ , ranging from 0.25  $\mu\text{g/L}$  for SMX to 1.25  $\mu\text{g/L}$  for DCF, except RAN which was never detected, and FUR and ACT reached, respectively,  $\sim 3$  and 15  $\mu\text{g/L}$  in one sample). The 7 pharmaceuticals were spiked in WW in order to detect them after oxidation and to calculate their removals. PFA was added to the sample at 5 different concentrations (1, 2, 5, 10, and 100 mg/L equivalent to 16, 32, 81, 161, and 1613  $\mu\text{M}$ ) under constant stirring.  $\text{Na}_2\text{S}_2\text{O}_3$  was added in excess after 1 h to stop the reaction before extraction and analysis (see Section 2.7). All experiments were conducted at least in duplicate.

## 2.7. Analytical Methods

Organic compounds used in kinetics experiments were quantified using high-performance liquid chromatography coupled to a diode array detection (HPLC-DAD, PD-M20A, Shimadzu). Analytical details (stationary and mobile phases elution gradient) are described in Text S3 (SI), and the operating wavelengths with maximum UV absorbance for all compounds are reported in Table S1 (SI).

The 7 pharmaceutical compounds spiked in WW effluent samples were analyzed by ultrahigh-performance liquid chromatography (UPLC) coupled with tandem mass spectrometry (MS/MS) with triple quadrupole detection (Acquity-TQD, Waters) after extraction using an automated solid-phase extraction (SPE) system (Dionex Autotrace 280, Thermo Scientific) with multilayer SPE cartridges as described previously.<sup>21,29</sup> Analytical details (stationary and mobile phases, internal standards, elution gradient, and ionization mode) and the MS/MS acquisition parameters are provided in SI (Text S3, Table S2).

The transformation products (TPs) were characterized by high-resolution mass spectrometry (HRMS) using UPLC coupled with ion mobility time-of-flight mass spectrometry (Vion IMS-QToF, Waters) and equipped with an ESI source. The analysis was performed in both negative and positive ionization modes, and mass spectra were acquired in HDMS<sup>E</sup> (data independent analysis) mode to obtain low and high collision energy fragments. All information regarding the instrument parameters and the method was published previously.<sup>21</sup>

### 3. RESULTS AND DISCUSSION

#### 3.1. Autodecomposition Kinetics of Peracids

Since PFA solutions are unstable, the autodecomposition rates of PFA and PAA were determined at different pH levels (ranging from 2.3 to 11.0) in PBS (prior experiments showed no influence of phosphate ion, Text S4) to understand their behavior in the absence of other compounds. All autodecomposition experiments followed first-order kinetics for both PFA (Figure 1) and PAA (Figure S2).

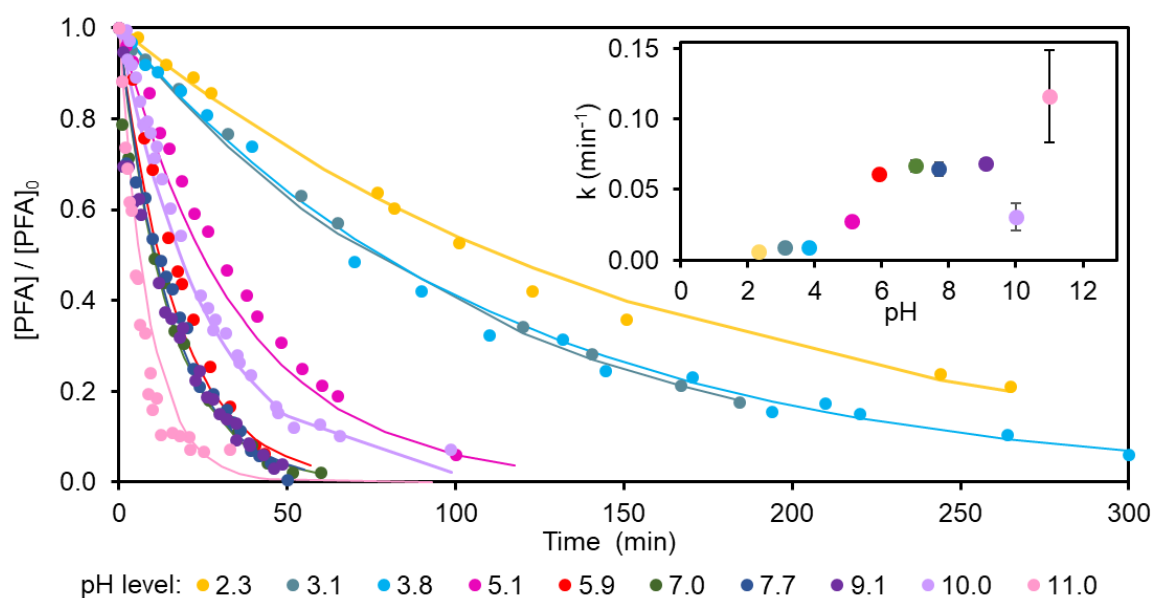


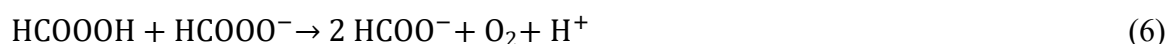
Figure 1. Autodecomposition of PFA in 10 mM phosphate buffer solution (PBS) at various initial pH levels, except for pH 3.8 representing the autodecomposition of PFA in DI water

without controlling pH (see Text S4).  $[PFA]_0 = 1.8 \pm 0.3$  mg/L ( $29 \mu\text{M}$ ). Errors bars on the rate constant values represent standard deviation from triplicate experiments.

The autodecomposition of PFA generally increased with increasing pH as reported for PAA,<sup>30,31</sup> showing similar decomposition rates between pH 5.9 and 9.1 and a decrease at pH 10.0 (Figure 1). The autodecomposition of PFA was much slower at acidic pH ( $k_{PFA} = 6.1 \times 10^{-3}$ ,  $9.3 \times 10^{-3}$ , and  $2.8 \times 10^{-2} \text{ min}^{-1}$  at pH 2.3, 3.1, and 5.1, respectively). Such a low degradation of PFA in acidic conditions and a higher degradation above pH 7.0 were reported in simulated combined sewer overflow waters.<sup>8</sup> This is in accordance with previous research showing that high acidity has a stabilizing effect on PFA.<sup>15</sup> In addition to its hydrolysis (reverse reaction in eq 1), PFA is generally considered to follow a decomposition reaction as described in eq 5.<sup>15,32,33</sup>



Kinetic modeling using eqs 1 and 5 could not explain the higher decomposition rates obtained near neutral pH and the restabilization at pH 10 because the kinetic constants proposed in the literature were obtained in acidic conditions (either with formic acid only or in the presence of sulfuric or phosphoric acid). The high decomposition rate observed in our study around the  $pK_a$  value of PFA ( $7.1^{7,34}$ ) was consistent with a spontaneous decomposition of PFA by reaction between its acidic form (PFAH) and its basic form ( $\text{PFA}^-$ ) (eq 6), as reported for PAA in several studies.<sup>31,35,36</sup>



The decrease in PFA decomposition at pH 10 can thus be explained by a lower presence of PFAH, limiting the occurrence of this reaction. Base-catalyzed reactions with hydroxide ions ( $\text{OH}^-$ ) or the presence of carbonate ions (from the dissolution of carbon dioxide in the solution)

however probably played a role in the higher decomposition rate observed at pH 11. Kinetic modeling was attempted by introducing such reactions and the speciation of carbonate and phosphate ions (Figure S3D and E), but some discrepancies remained between the model and the experimental data (Table S3, Figure S4). Further research would be needed to fully elucidate the role of all present species and to provide a comprehensive kinetic model. In contrast to PFA, PAA was stable in both acidic and neutral pH conditions, and its lower autodecomposition was confirmed at pH 7.7 ( $k_{\text{PAA}} = 3.1 \times 10^{-3} \text{ min}^{-1}$  and  $k_{\text{PFA}} = 6.5 \times 10^{-2} \text{ min}^{-1}$ ) and at pH 5.9 ( $k_{\text{PAA}} = 3.6 \times 10^{-3} \text{ min}^{-1}$  and  $k_{\text{PFA}} = 6.5 \times 10^{-2} \text{ min}^{-1}$ ) (Figure S2). This result agrees with previous findings that demonstrate the low decomposition of PAA in the pH range of 5.5 to 8.2.<sup>30</sup> In these experiments performed in DI water, the high stability of PAA compared to PFA can be attributed to its longer carbon chain, as aliphatic peracids tend to become more stable with longer chain lengths.<sup>37</sup>

### 3.2. Reactivity of PFA with Inorganic and Organic Compounds

The reactivity of PFA with inorganic and organic compounds was first assessed by measuring the consumption of PFA by various compounds after 10 min of reaction to quickly identify the most reactive chemical structures. The PFA consumption results were expressed as residual concentration ratio (RCR, i.e., PFA residual normalized with the PFA autodecomposition).

Among the 7 inorganic ions studied (i.e., ammonia nitrogen, nitrite, bromide, iodide, chloride, iron(II) and hydrogen phosphate ions), only iodide ion consumed PFA in PBS (Figure S5). In DI water, reduced iron ( $\text{Fe}^{2+}$ ) exhibited a different reactivity, consuming around 20% of PFA (Figure S5). The difference in PFA consumption in PBS (pH 7.0) and DI water (pH 7.1) for  $\text{Fe}^{2+}$  suggests that hydrogen phosphate ion can act as a chelating compound and decrease the consumption of PFA by  $\text{Fe}^{2+}$ . This effect has also been observed for PAA (DI water, pH 7.5),

where the presence of hydrogen phosphate ions decreased the impact of  $\text{Fe}^{2+}$  on PAA decomposition.<sup>27</sup>

Among the 9 amino acids, cysteine, methionine, and, to a lesser extent, tryptophan were the most reactive with PFA (Figure 2A). PFA was completely consumed by cysteine ( $\text{RCR} = 0$ ), which is consistent with the high reactivity of cysteine with PAA<sup>38</sup> and the recent findings by Wang et al.,<sup>39</sup> showing the higher reactivity of cysteine and methionine with PFA. The reactivity of tryptophan with PFA is also in agreement with the reactivity of protein-like compounds (such as tryptophan and tyrosine) measured by fluorescence spectroscopy during the disinfection of WW.<sup>6</sup> In addition, the lack of PFA consumption by tyrosine, glutamine, histidine, and glycine, indicating their lower reactivity, is consistent with the results of Wang et al.,<sup>39</sup> who reported rate constants lower than  $0.1 \text{ M}^{-1} \text{ s}^{-1}$  for these amino acids at neutral pH (7.1).

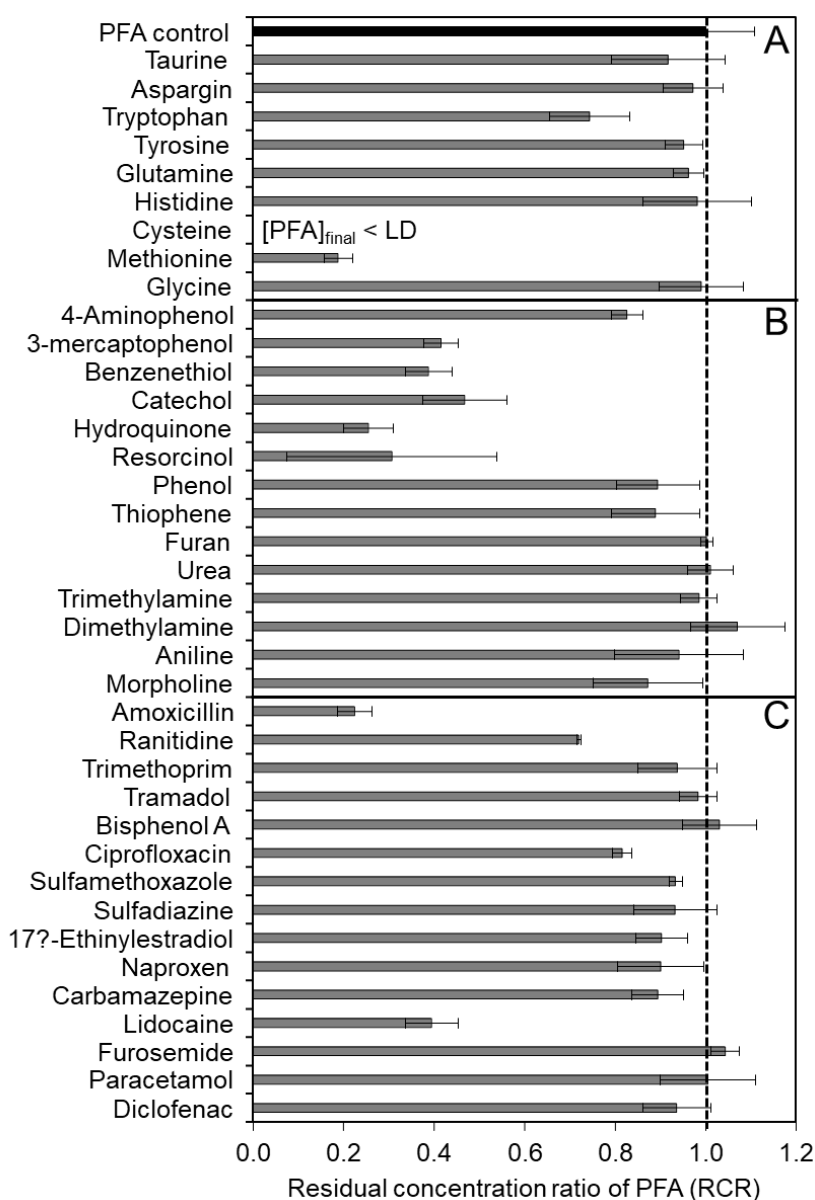


Figure 2. Relative consumption of 16  $\mu\text{M}$  of PFA by 8  $\mu\text{M}$  amino acids (A), model organic compounds (B), and pharmaceutical compounds (C) at pH 7.0,  $20.0 \pm 1.0$   $^{\circ}\text{C}$ , and 10 min of reaction time. Results expressed as residual concentration ratio (RCR). The black bar corresponds to the RCR of PFA self-decomposition (RCR = 1), and gray bars correspond to the RCR of PFA in the presence of an organic compound. Values close to zero (as for cysteine) indicate significant consumption of PFA.  $[\text{PFA}]_{\text{final}} < \text{LD}$  means that the residual concentration of PFA is lower than the detection limit after 10 min of reaction.

PFA reacted with 9 of the 14 model organic compounds: resorcinol, hydroquinone, benzenethiol, 3-mercaptophenol, 4-aminophenol, thiophene, morpholine, aniline and phenol (Figure 2B). The reactivity of metalloles (derivatives of cyclopentadiene in which a carbon atom is replaced by a heteroatom) increased when they contained a sulfur heteroatom instead of an oxygen heteroatom (i.e., thiophene compared to furan). The strong reactivity of thiophene with PAA has been previously demonstrated during the oxidation of subbituminous carbons, resulting in the formation of sulfate ions or sulphone compounds.<sup>40</sup> PFA was slightly consumed by phenol and very slightly by aniline (considering the standard deviation of RCR results). The reactivity of substituted benzenic compounds largely increased with the addition of a second electron-donating group such as hydroxyl (–OH) (resorcinol, hydroquinone, and catechol compared to phenol, and 4-aminophenol compared to aniline). The presence of a thiol group (–SH) instead of hydroxyl (–OH) also dramatically increased the reactivity of the molecule (benzenethiol compared to phenol) but the addition of another –OH group to benzenethiol (3-mercaptophenol) did not increase its reactivity.

Out of the 15 pharmaceutical compounds investigated, 8 were found to react with PFA: amoxicillin, ranitidine, ciprofloxacin, sulfamethoxazole, sulfadiazine, 17 $\alpha$ -ethinylestradiol, carbamazepine, and lidocaine (Figure 2C). For naproxen and trimethoprim, no significant PFA consumption was observed given the variability of the results. PFA weakly reacted with some aromatic and amide compounds (e.g., 17 $\alpha$ -ethinylestradiol and carbamazepine) as well as compounds containing aromatic amine groups (e.g., sulfamethoxazole and sulfadiazine), in accordance with the results obtained with aniline. This reactivity of aromatic amine compounds was also demonstrated for PAA, with an oxygen attack occurring on the aromatic ring.<sup>41</sup> PFA was highly reactive with other organic compounds containing reduced-sulfur or nitrogen moieties (e.g., amoxicillin, ranitidine, and lidocaine). The high consumption of PFA by lidocaine is in accordance with a previous study and can be attributed to the reactivity of the



307 deprotonated tertiary amine group to form lidocaine N-oxide.<sup>21</sup> In contrast, the very low  
308 reactivity of tramadol, which also has a tertiary amine group, can be attributed to the absence  
309 of its deprotonated form at pH 7.0 ( $pK_a = 9.23$ ).<sup>21</sup> Carbamazepine, another compound with a  
310 tertiary amine moiety in a non-protonated form, also showed low consumption of PFA. This  
311 can be attributed to the higher stability of the nitrogen atom in the tertiary amine group due to  
312 steric hindrance and/or the electron-withdrawing effect of the aromatic rings and the carbonyl  
313 group.<sup>42</sup> The moderate consumption of PFA by ciprofloxacin can be explained by its secondary  
314 amine heteroatom group similar to morpholine that showed comparable consumption of PFA.  
315 Ciprofloxacin also has tertiary amine groups but similar to carbamazepine, they were probably  
316 not reactive due to their high stability and inability to be protonated (no  $pK_a$  on these nitrogen  
317 atoms) or attacked by oxygen. Compounds containing secondary amine groups (e.g.,  
318 diclofenac, acetaminophen, sulfadiazine, furosemide, or trimethoprim) did not consume or were  
319 very weakly reactive with PFA, which can be explained by similar stabilization effects.  
320 Dimethylamine and trimethylamine also did not consume any significant amount of PFA,  
321 indicating that N-oxide formation requires the presence of groups that destabilize the molecule  
322 (e.g., electron-donating groups). Given the low reactivity of PFA with phenol and  
323 primary/secondary amines, the high reactivity of amoxicillin should be attributed to other  
324 functional groups such as the thioether sulfur heteroatom. The reactivity of this thioether group  
325 of  $\beta$ -lactams has been demonstrated with PAA, generating sulfoxide products.<sup>43</sup> Taking into  
326 account all these results, the moderate consumption of PFA by ranitidine could be explained by  
327 the reactivity of both its thioether and deprotonated tertiary amine groups. Taurine, sulfadiazine  
328 and sulfamethoxazole, while sulfur-containing, have a fully oxidized sulfur atom (i.e., sulfonyl  
329 moiety,  $O=S=O$ ), which results in their very low PFA consumption, as previously reported for  
330 their reactivity with PAA.<sup>41</sup>

These results especially demonstrate the high reactivity of compounds containing reduced-sulfur moieties such as thiol and thioether groups (cysteine, methionine, benzenethiol, 3-mercaptophenol, amoxicillin, and ranitidine), as well as deprotonated tertiary amine groups destabilized by electron-donating groups. This reactivity follows similar trends as that of ozone since it has been demonstrated that tertiary amines have a higher reactivity with ozone than secondary amines due to the inductive effects of alkyl groups and also that the deprotonated form of amines is generally more reactive than the protonated form.<sup>42,44</sup>

### 3.3. Kinetics of Organic Compound Oxidation by PFA

Since PFA consumption could be biased by the presence of transformation products (TPs) with potential PFA reactivity, further experiments were carried out to study the oxidation kinetics of 13 organic compounds (chosen among model and pharmaceutical compounds) by monitoring their degradation. A control experiment revealed that there was no significant difference in PFA consumption in the presence or absence of the organic compound (Figure S6). This supports the assumption of pseudo-first-order kinetics with respect to the organic compound and shows that in these conditions, PFA remained in excess and its degradation was mainly due to its autodecomposition (i.e., negligible consumption by organic compounds). Other control experiments also showed no contribution of background  $\text{H}_2\text{O}_2$  concentration to the degradation of organic compounds (Text S5).

#### 3.3.1. Kinetic Constants of Model Compounds

The kinetic constants of 6 model organic compounds, containing only one aromatic ring, were determined (Table 1). The compounds included 2 sulfur molecules containing thiol groups (benzenethiol and 3-mercaptophenol) and 4 phenolic molecules (phenol, resorcinol, hydroquinone, and catechol). The kinetic reactivities followed similar trends to PFA consumptions (Section 3.2), with sulfur molecules and benzenediols showing higher reactivity

compared to simple phenol. PFA completely oxidized benzenethiol and 3-mercaptophenol in less than 1 min (Table S4) so their rate constants ( $k_{\text{PFA}}$ ) were estimated to be greater than  $2 \times 10^2 \text{ M}^{-1} \text{ s}^{-1}$ . The reactions of the 4 phenolic compounds followed second-order kinetics with respect to both the organic compound and PFA concentrations. Their apparent rate constants ( $k_{\text{app}}$ ) ranged from  $0.04 \pm 0.01$  to  $3.04 \pm 0.06 \text{ M}^{-1} \text{ s}^{-1}$  at pH 7.0, with phenol being the least reactive and catechol the most reactive molecule. The kinetic rate constants of the various types of benzenediols showed clear differences depending on the position of  $-\text{OH}$  substituents despite similar PFA consumption observed for them (Table 1 and Figure 2B). This confirms that adding a second  $-\text{OH}$  substituent to phenol plays a crucial role in the reactivity of phenolic compounds with PFA but also reveals that its relative position influences the oxidation rate. The ortho position of the  $-\text{OH}$  group in catechol enhanced its reactivity compared to hydroquinone (para position) and resorcinol (meta position). The enhanced reactivity of phenolic compounds containing multiple  $-\text{OH}$  substituents can be attributed to an increase in electron density from electron-donating groups, as previously observed for PAA.<sup>41</sup> The reported  $k_{\text{PAA}}$  values for phenol and catechol ( $0.08 \pm 0.04$  and  $33.00 \pm 0.40 \text{ M}^{-1} \text{ s}^{-1}$  at pH 5, respectively<sup>41</sup>) were in the same range as  $k_{\text{PFA}}$  ( $0.04 \pm 0.01$  and  $3.04 \pm 0.06$  at pH 7.0, respectively) (Table 1).

### 3.3.2. Kinetic Constants of Pharmaceutical Compounds

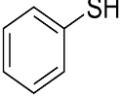
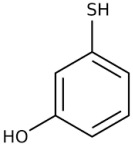
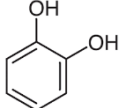
The kinetics of 7 pharmaceutical compounds were studied (Table 1): ranitidine (RAN), lidocaine (LID), furosemide (FUR), diclofenac (DCF), acetaminophen (ACT), sulfamethoxazole (SMX), and carbamazepine (CBZ). Similar to PFA consumption, the highest reactivities were observed for compounds containing reduced-sulfur and deprotonated amine moieties. RAN (containing a thioether and a tertiary amine group) was fully degraded by PFA in less than 30 seconds, so its  $k_{\text{PFA}}$  was estimated to be greater than  $2 \times 10^3 \text{ M}^{-1} \text{ s}^{-1}$ . LID and FUR (two secondary amines with no reduced-sulfur group) were moderately degraded with  $k_{\text{PFA}}$  values of  $2.24 \pm 0.14$  and  $0.41 \pm 0.18 \text{ M}^{-1} \text{ s}^{-1}$ , respectively. A similar kinetic rate constant

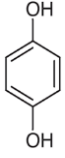
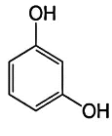
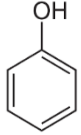
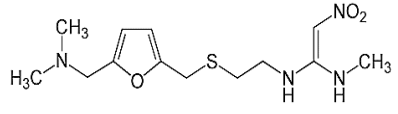
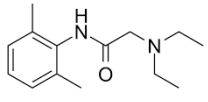
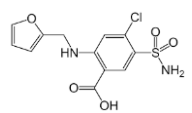
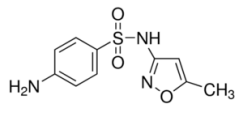
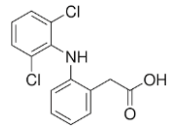
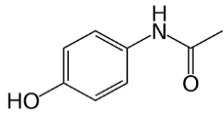
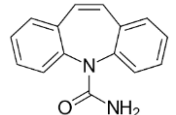
was obtained for LID in a previous study ( $k_{\text{PFA}} = 2.76 \pm 0.37 \text{ M}^{-1} \text{ s}^{-1}$  at pH 7.0).<sup>21</sup> Additional experiments performed with FUR confirmed the increase of its  $k_{\text{obs}}$  with increasing PFA concentrations, in accordance with second-order oxidation kinetics (Text S6, Figure S7). Three other pharmaceutical compounds (SMX, DCF, ACT) exhibited weaker reactivity with PFA (kinetic rate constants in the range from 0.11 to  $0.14 \pm 0.02 \text{ M}^{-1} \text{ s}^{-1}$ ), in the same range as those observed for simple phenolic molecules (Table 1). CBZ was the least reactive compound, with a rate constant of  $7.15 \pm 0.97 \times 10^{-3} \text{ M}^{-1} \text{ s}^{-1}$ . Different trends between oxidation rate constants were observed compared to the PFA consumption of the same molecules (i.e., a lower PFA consumption of RAN than that of LID and a similar or even higher PFA consumption for CBZ than those of SMX, DCF, ACT, and FUR). As mentioned earlier, PFA consumption of some molecules could be increased by the formation of more reactive TPs, while some highly reactive molecules (e.g., RAN) could form less-reactive TPs resulting in decreased PFA consumption.

Similar to these results obtained with PFA, the high reactivity of reduced-sulfur compounds (e.g., cysteine and methionine) with PAA has been described, with  $k_{\text{PAA}}$  values ranging from  $\sim 5$  to  $> 6 \times 10^2 \text{ M}^{-1} \text{ s}^{-1}$ .<sup>38</sup> The kinetic rate constants of cysteine and methionine have recently been evaluated for both PFA and PAA, with values reaching  $> 1 \times 10^5 \text{ M}^{-1} \text{ s}^{-1}$ .<sup>39</sup> This was attributed to the strong susceptibility of the reduced sulfur atom to electrophilic attack, corresponding to an electron transfer mechanism.<sup>38,39</sup> The  $k_{\text{PFA}}$  values of CBZ, SMX, DCF, ACT, FUR, and LID were in the same range as the  $k_{\text{PAA}}$  values reported for similar nitrogen-containing compounds (from  $2.5 \times 10^{-3}$  to  $1.6 \times 10^1 \text{ M}^{-1} \text{ s}^{-1}$ ).<sup>41</sup> The  $k_{\text{PFA}}$  of some investigated pharmaceutical compounds (SMX and DCF) were about 100 times higher than their reported  $k_{\text{PAA}}$  values (Table 1).<sup>41</sup> Some other molecules exhibited lower reactivity with PFA than with PAA (i.e., 5 times lower  $k_{\text{PFA}}$  for CBZ, 10 times lower  $k_{\text{PFA}}$  for catechol, and a slightly lower  $k_{\text{PFA}}$  for phenol). This suggests that PFA and PAA globally share similar reaction pathways for certain types of molecular groups, but the oxidation power of PFA can vary greatly depending

on the targeted molecule, being either lower or higher than that of PAA. This reactivity difference could also be due to the pH values, as the  $k_{\text{PAA}}$  values were reported at pH 5.0,<sup>41</sup> while the pH level in the present study was 7.0. Other differences in experimental conditions (e.g., different buffer species, different ratios between reactive species, or the presence of unknown reactive species formed during the degradation of peracids) could also play a role in these different behaviors. Kinetics of LID and DCF decomposition at different pH showed a much stronger reactivity at neutral or alkaline pH, suggesting a major role of the PFA deprotonated form ( $\text{PFA}^-$ ) (Text S7, Figures S3, S8). An even more diverse set of molecular structures should be investigated to fully understand the reactivity of PFA and potentially predict the kinetic rates of organic molecules (e.g., with quantitative structure–activity relationship models). Overall, PFA was found to be less oxidative than ozone toward the studied pharmaceuticals, as indicated by the significantly higher kinetic rate constants reported in the literature for ozone (from  $10^4$  to  $>10^6 \text{ M}^{-1} \text{ s}^{-1}$ ).<sup>45,46</sup>

Table 1. Second-Order Rate Constants ( $k_{\text{app}}$ ,  $\text{M}^{-1} \text{ s}^{-1}$ ) of Model Organic and Pharmaceutical Compounds Oxidation by PFA. Experimental conditions:  $[\text{compound}]_0 = 1 \text{ } \mu\text{M}$ ,  $[\text{PFA}]_0 = 500 \text{ } \mu\text{M}$ .  $k_{\text{PAA}}$  from Kim &Huang<sup>41</sup> at pH 5.0 and 22.0 °C.

compounds	structure	$k_{\text{PFA}} (\text{M}^{-1} \text{ s}^{-1})$	$k_{\text{PAA}} (\text{M}^{-1} \text{ s}^{-1})$
benzenethiol		$> 2 \times 10^2$	
3-mercaptophenol		$> 2 \times 10^2$	
catechol		$3.04 \pm 0.06$	$3.33 \pm 0.40 \times 10^1$

hydroquinone		$0.80 \pm 0.21$	
resorcinol		$0.10 \pm 0.02$	
phenol		$0.04 \pm 0.01$	$8.00 \pm 0.40 \times 10^{-2}$
ranitidine		$> 2 \times 10^3$	
lidocaine		$2.24 \pm 0.14$	
furosemide		$0.41 \pm 0.18$	
sulfamethoxazole		$0.14 \pm 0.02$	$3.7 \pm 0.10 \times 10^{-3}$
diclofenac		$0.13 \pm 0.03$	$3.1 \pm 0.80 \times 10^{-3}$
acetaminophen		$0.11 \pm 0.02$	
carbamazepine		$7.15 \pm 0.97 \times 10^{-3}$	$3.4 \pm 0.40 \times 10^{-2}$

422

423 3.4. Influence of the PFA Dose in Environmental Water Matrices

424 The reactivity of the 7 pharmaceuticals for which oxidation kinetics are determined in Section

425 3.3 (RAN, LID, FUR, SMX, DCF, ACT, and CBZ) was investigated in real WW effluent to

assess the effect of the WW matrix. The water quality parameters of the WW sample were described in Section 2.6.

The removal of the chosen micropollutants in real WW was low and very selective. RAN was the best-eliminated compound, and its removal increased from 10 to 99% when the PFA concentration varied between 1 and 100 mg/L (16 to 1613  $\mu$ M) (Figure 3). CBZ, ACT, and DCF were recalcitrant to PFA oxidation, showing low removals (<10%) at all concentrations. SMX also exhibited low removals, but some increase was observed at 100 mg/L (1613  $\mu$ M), reaching ~18%. FUR and LID were slightly removed at PFA concentrations <5 mg/L (81  $\mu$ M) and their removal significantly increased at higher concentrations. Contrary to RAN, their removal did not exceed 35% even at the highest concentrations. In addition, a slightly negative removal (−5%) was obtained for FUR at a 1 mg/L PFA concentration, which can be considered as not significant due to analytical uncertainties (e.g., discrepancies in the extraction of internal standards and matrix effects), especially at low concentrations of micropollutants.

Overall, even though most pharmaceuticals exhibited lower removals than expected after 1 h based on their oxidation rate constants in PBS, their reactivities in WW followed the same trends (Section 3.3), with RAN being the most reactive compound followed by LID and FUR. In PBS and at pH 7.0, 1  $\mu$ M of LID and FUR resulted in  $91 \pm 1$  and  $38 \pm 10\%$  removal, respectively, with 31 mg/L (500  $\mu$ M) of PFA (Figure S9). At 100 mg/L (1613  $\mu$ M) of PFA and at the pH of the WW effluent (7.9), it was expected that their removal rates would be even higher especially since LID has been found to be more reactive at pH 8.0 than at pH 7.0 ( $k_{app}$  of  $2.24 \pm 0.14$  and  $7.54 \pm 0.90$   $M^{-1} s^{-1}$  at pH 7.0 and 8.0, respectively).<sup>21</sup> The decrease of organic micropollutants (OMP) removal in real WW can be related to the presence of total suspended solids (TSS), organic matter (OM), and other species that could consume PFA (e.g., transition metals such as  $Fe^{2+}$ ,  $Cu^{2+}$ , and  $Mn^{2+}$ ) and thus compete with the OMP removal. More

systematic experiments (e.g., with synthetic OM) are needed to understand such competition effects during PFA oxidation.

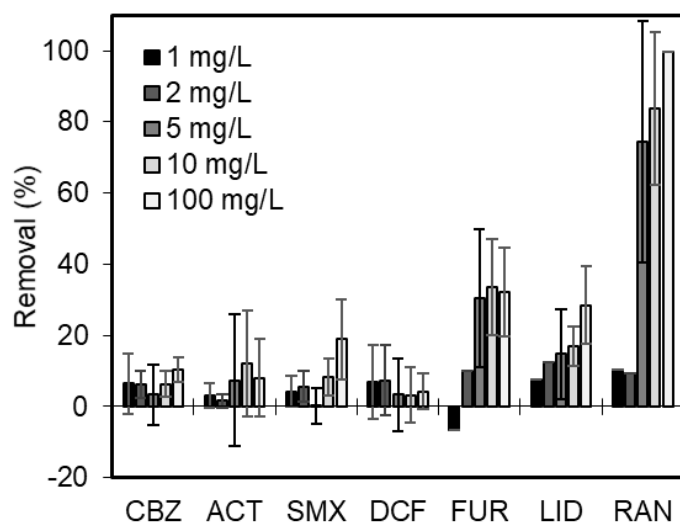


Figure 3. Removal of pharmaceuticals in wastewater by PFA. Experimental conditions: [Pharmaceutical compound]<sub>0</sub> = C<sub>0</sub> + 1 µg/L ( $\sim 4 \times 10^{-3}$  µM) spiked in WW, with C<sub>0</sub>, the initial concentration of the compound in the WW effluent, reaction time = 60 min, pH = 7.88 ± 0.10, 20.0 °C, [PFA]<sub>0</sub> = 1, 2, 5, 10, and 100 mg/L (16, 32, 81, 161, 1613 µM). Error bars represent the standard deviation from triplicate samples.

### 3.5. Identification of Oxidation Byproducts

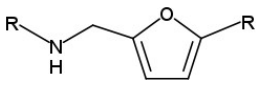
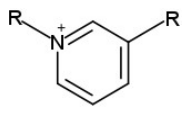
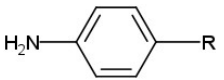
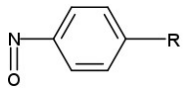
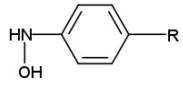
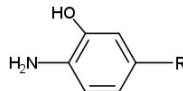
To better understand the oxidation mechanisms of organic compounds by PFA, TPs produced by the reaction between PFA and individual solutions of organic compounds in 10 mM PBS (pH 7.0) were characterized by HRMS. Among the model organic compounds (Sections 3.2 and 3.3), only benzenethiol (BZT), 3-mercaptophenol (3MP), and catechol (CTL) were studied, as the other compounds or their TPs were not adequately detected. The exact masses of the parent compounds and their TPs, as well as their detection parameters and main fragments, are



described in Tables S5 and S6, and the detailed identifications for each parent compound are described in Text S8 (SI).

For both model organic and pharmaceutical compounds, the addition of oxygen atoms on specific functional groups (such as thioether, thiol, and tertiary amine) was the major mechanism observed, with N-oxides, S-oxides, or hydroxylated compounds being the main observed types of TPs (Table 2). The oxidation of thiol compounds (BZT and 3MP) resulted in the addition of three oxygen atoms (i.e., sulfonic acid compounds), and the oxidation of the thioether group in RAN formed the S-oxide (1 additional oxygen atom) and sulfonyl (2 oxygen atoms) analogues. Compounds containing tertiary amine groups (RAN and LID) formed N-oxides (as previously reported for LID<sup>21</sup>), and SMX (aniline moiety) formed hydroxylated TPs. Similar mechanisms were reported for PAA oxidation<sup>38,41,43,47</sup> and ozonation,<sup>48,49</sup> suggesting similar sites of attack by these three oxidants. This is also in accordance with the higher reactivity of compounds containing reduced-sulfur or amine molecular groups (Sections 3.2 and 3.3). The TPs of SMX confirmed that aniline is a reactive site, even if its reactivity is very weak (considering the low consumption of PFA by SMX, sulfadiazine and aniline itself). Other TPs with no addition of oxygen but a rearrangement of aromatic rings (pyridiniums) were also detected from FUR and RAN. The formation of pyridinium of FUR was previously reported during anodic oxidation or with electro-Fenton process.<sup>50,51</sup> The TPs identified in this study were chemically similar to their parent compounds, and almost no TPs of lower mass could be detected. This indicates a low transformation effect of PFA even for the most reactive compounds (i.e., sulfur-containing compounds such as RAN, BZT or 3MP), leading to their low mineralization. This should however be confirmed with other analytical techniques to target smaller, more polar or more volatile TPs (e.g., gas chromatography coupled to mass spectrometry).

Table 2. Reactive Sites of the Studied Organic Compounds with the Possible Pathways and Produced Byproducts for PFA Oxidation, from the Most Reactive (1) to the Least Reactive (4) Site (Based on Kinetic Constants Shown in Table 1).

reactive site of studied organic compounds	reactive site structure	reaction mechanism	possible oxidation byproducts (OBPs)
(1) reduced-sulfur moiety (thiol and thioether) (e.g., 3MP, BZT, RAN)	$\text{R}-\text{SH}$ $\text{R}-\text{S}-\text{R}$	O addition	$\text{R}-\text{S}(=\text{O})_2-\text{OH}$ $\text{R}-\text{S}(=\text{O})-\text{R}$ $\text{R}-\text{S}(=\text{O})_2-\text{R}$
(2) tertiary amine (e.g., LID, RAN)	$\text{R}-\text{N}(\text{R})_2$	O addition	$\text{R}-\text{N}^+(\text{R})_2-\text{O}^-$
(3) furan ring with secondary amine at the benzylic position (e.g., FUR, demethylated RAN)		ring rearrangement	
(4) aniline (e.g., SMX)		O addition, hydroxylation	  

N-oxides are known to be persistent and not biodegradable,<sup>44,52</sup> and some aromatic N-oxides have been shown to induce genotoxicity or to be potential carcinogens.<sup>53,54</sup> The stability and persistence of other main TPs produced from PFA (S-oxide, sulfonyl compounds) should thus

be evaluated to assess their potential impact in comparison to their parent molecules as well as their respective toxicity.

#### 4. ENVIRONMENTAL IMPLICATIONS

The increasing implementation of PFA disinfection units in WWTPs highlights the need to understand the effect of PFA on inorganic and organic compounds as well as its behavior under various conditions (e.g., pH, presence of OM). Autodecomposition experiments revealed that PFA was more stable in acidic conditions compared to neutral or alkaline conditions. Conversely, the oxidation of DCF and LID was more effective in alkaline conditions. The influence of the deprotonated form of PFA ( $\text{PFA}^-$ ) and its enhanced oxidation power while experiencing higher autodecomposition requires further investigation. Systematic PFA decomposition studies are still lacking to provide a comprehensive kinetic model that accurately reflects the behavior of PFA at various pH levels.

Major inorganic ions (such as ammonium, nitrite, bromide, chloride, and orthophosphate ions) did not consume PFA, indicating a low impact on the optimal dose of PFA to be used in WWTPs. PFA demonstrated a high selectivity towards specific organic moieties (e.g., reduced sulfur and tertiary amines), with apparent low transformation and mineralization of organic compounds, even for highly reactive ones (i.e., sulfur-containing compounds such as ranitidine, benzenethiol, or 3-mercaptophenol). This suggests a low concern for the formation of numerous and toxic TP<sub>s</sub> during PFA disinfection as compared to other oxidation processes. However, it is crucial to evaluate the stability, persistence, and potential toxicity of S-oxides, sulfonyl, or N-oxides compounds in the environment to assess their impact compared to their parent molecules. The high selectivity of PFA toward reduced sulfur is also consistent with recent findings showing its high reactivity with cysteine and methionine, responsible for its specific disinfection properties (i.e., bacterial inactivation through accumulation in cells and intracellular oxidation).<sup>39</sup>

Due to the presence of TSS, OM and/or transition metals, pharmaceutical compounds were less effectively eliminated in real WW compared to PBS. The impact of TSS has been observed on PFA disinfection,<sup>6</sup> but it would require further investigation regarding oxidation reactions as well as the competition between OM and micropollutants.

Overall, PFA does not appear to be an efficient oxidant for the advanced treatment of micropollutants. Therefore, future research could focus on its activation (e.g., through irradiation or metals) to enhance the removal of organic compounds while still utilizing its advantages in disinfection.

## SUPPORTING INFORMATION

The Supporting Information is available free of charge e at

<https://pubs.acs.org/doi/10.1021/acsestwater.3c00279>.

Additional analytical details, effect of several parameters (phosphate ion, background H<sub>2</sub>O<sub>2</sub> concentration, PFA initial concentration, pH) on PFA autodecomposition and oxidation kinetics, additional kinetics results, species distribution diagrams of PFA and selected micropollutants or inorganic ions, HRMS detailed identifications and the corresponding reaction pathways, and HRMS spectra of micropollutants and their transformation products.

## NOTES

The authors declare no competing financial interest.

## ACKNOWLEDGMENTS

This work was conducted as part of the OPUR research program and received partial support from the WaterOmics program (ANR-17-CE34-0009-01). The authors also acknowledge the PRAMMICS Platform (OSU-EFLUVE UMS 3563) for their assistance with UPLC-IMS-

547 QTOF and HPLC-DAD analysis, Michael Rivard for synthesizing and providing pyridinium of  
 548 furosemide, Maysar Bouslah, Melissia Ben-Iken, and Ilyess Taibi for their contributions to the  
 549 experiments, and Lila Boudahmane for her assistance with laboratory experiments.

## 550 REFERENCES

- 551 (1) Campo, N.; De Flora, C.; Maffettone, R.; Manoli, K.; Sarathy, S.; Santoro, D.;  
 552 Gonzalez-Olmos, R.; Auset, M. Inactivation Kinetics of Antibiotic Resistant Escherichia Coli  
 553 in Secondary Wastewater Effluents by Peracetic and Performic Acids. *Water Research* **2020**,  
 554 *169*, 115227. <https://doi.org/10.1016/j.watres.2019.115227>.
- 555 (2) Gehr, R.; Chen, D.; Moreau, M. Performic Acid (PFA): Tests on an Advanced Primary  
 556 Effluent Show Promising Disinfection Performance. *Water Science and Technology* **2009**, *59*  
 557 (1), 89–96. <https://doi.org/10.2166/wst.2009.761>.
- 558 (3) Karpova, T.; Pekonen, P.; Gramstad, R.; Öjstedt, U.; Laborda, S.; Heinonen-Tanski, H.;  
 559 Chávez, A.; Jiménez, B. Performic Acid for Advanced Wastewater Disinfection. *Water Sci*  
 560 *Technol* **2013**, *68* (9), 2090–2096. <https://doi.org/10.2166/wst.2013.468>.
- 561 (4) Kitis, M. Disinfection of Wastewater with Peracetic Acid: A Review. *Environment*  
 562 *International* **2004**, *30* (1), 47–55. [https://doi.org/10.1016/S0160-4120\(03\)00147-8](https://doi.org/10.1016/S0160-4120(03)00147-8).
- 563 (5) Ragazzo, P.; Chiucchini, N.; Piccolo, V.; Spadolini, M.; Carrer, S.; Zanon, F.; Gehr, R.  
 564 Wastewater Disinfection: Long-Term Laboratory and Full-Scale Studies on Performic Acid in  
 565 Comparison with Peracetic Acid and Chlorine. *Water Research* **2020**, *184*, 116169.  
 566 <https://doi.org/10.1016/j.watres.2020.116169>.
- 567 (6) *Effectiveness of Disinfecting Wastewater Treatment Plant Discharges: Case of*  
 568 *Chemical Disinfection Using Performic Acid*; Rocher, V., Azimi, S., Eds.; IWA Publishing,  
 569 2021. <https://doi.org/10.2166/9781789062106>.
- 570 (7) Luukkonen, T.; Heyninck, T.; Rämö, J.; Lassi, U. Comparison of Organic Peracids in  
 571 Wastewater Treatment: Disinfection, Oxidation and Corrosion. *Water Research* **2015**, *85*, 275–  
 572 285. <https://doi.org/10.1016/j.watres.2015.08.037>.
- 573 (8) Chhetri, R. K.; Thornberg, D.; Berner, J.; Öjstedt, U.; Sharma, A. K.; Andersen, H. R.;  
 574 Andersen, H. R. Chemical Disinfection of Combined Sewer Overflow Waters Using Performic  
 575 Acid or Peracetic Acids. *Science of The Total Environment* **2014**, *490*, 1065–1072.  
 576 <https://doi.org/10.1016/j.scitotenv.2014.05.079>.
- 577 (9) Chhetri, R. K.; Flagstad, R.; Munch, E. S.; Hørning, C.; Berner, J.; Kolte-Olsen, A.;  
 578 Thornberg, D.; Andersen, H. R. Full Scale Evaluation of Combined Sewer Overflows  
 579 Disinfection Using Performic Acid in a Sea-Outfall Pipe. *Chemical Engineering Journal* **2015**,  
 580 *270*, 133–139. <https://doi.org/10.1016/j.cej.2015.01.136>.
- 581 (10) Chhetri, R. K.; Baun, A.; Andersen, H. R. Algal Toxicity of the Alternative  
 582 Disinfectants Performic Acid (PFA), Peracetic Acid (PAA), Chlorine Dioxide (ClO<sub>2</sub>) and  
 583 Their by-Products Hydrogen Peroxide (H<sub>2</sub>O<sub>2</sub>) and Chlorite (ClO<sub>2</sub><sup>-</sup>). *International Journal*  
 584 *of Hygiene and Environmental Health* **2017**, *220* (3), 570–574.  
 585 <https://doi.org/10.1016/j.ijheh.2016.11.011>.

- 586 (11) Guzzella, L.; Monarca, S.; Zani, C.; Feretti, D.; Zerbini, I.; Buschini, A.; Poli, P.; Rossi,  
587 C.; Richardson, S. D. In Vitro Potential Genotoxic Effects of Surface Drinking Water Treated  
588 with Chlorine and Alternative Disinfectants. *Mutation Research/Genetic Toxicology and*  
589 *Environmental Mutagenesis* **2004**, *564* (2), 179–193.  
590 <https://doi.org/10.1016/j.mrgentox.2004.08.006>.
- 591 (12) Dell’Erba, A.; Falsanisi, D.; Liberti, L.; Notarnicola, M.; Santoro, D. Disinfection By-  
592 Products Formation during Wastewater Disinfection with Peracetic Acid. *Desalination* **2007**,  
593 *215* (1), 177–186. <https://doi.org/10.1016/j.desal.2006.08.021>.
- 594 (13) Ragazzo, P.; Chiucchini, N.; Piccolo, V.; Ostoich, M. A New Disinfection System for  
595 Wastewater Treatment: Performic Acid Full-Scale Trial Evaluations. *Water Science and*  
596 *Technology* **2013**, *67* (11), 2476–2487. <https://doi.org/10.2166/wst.2013.137>.
- 597 (14) Ragazzo, P.; Feretti, D.; Monarca, S.; Dominici, L.; Ceretti, E.; Viola, G.; Piccolo, V.;  
598 Chiucchini, N.; Villarini, M. Evaluation of Cytotoxicity, Genotoxicity, and Apoptosis of  
599 Wastewater before and after Disinfection with Performic Acid. *Water Research* **2017**, *116*, 44–  
600 52. <https://doi.org/10.1016/j.watres.2017.03.016>.
- 601 (15) Santacesaria, E.; Russo, V.; Tesser, R.; Turco, R.; Di Serio, M. Kinetics of Performic  
602 Acid Synthesis and Decomposition. *Ind. Eng. Chem. Res.* **2017**, *56* (45), 12940–12952.  
603 <https://doi.org/10.1021/acs.iecr.7b00593>.
- 604 (16) Luukkonen, T.; Pehkonen, S. O. Peracids in Water Treatment: A Critical Review.  
605 *Critical Reviews in Environmental Science and Technology* **2017**, *47* (1), 1–39.  
606 <https://doi.org/10.1080/10643389.2016.1272343>.
- 607 (17) Zhang, C.; Brown, P. J. B.; Hu, Z. Thermodynamic Properties of an Emerging Chemical  
608 Disinfectant, Peracetic Acid. *Science of The Total Environment* **2018**, *621*, 948–959.  
609 <https://doi.org/10.1016/j.scitotenv.2017.10.195>.
- 610 (18) Gagnon, C.; Lajeunesse, A.; Cejka, P.; Gagné, F.; Hausler, R. Degradation of Selected  
611 Acidic and Neutral Pharmaceutical Products in a Primary-Treated Wastewater by Disinfection  
612 Processes. *Ozone: Science & Engineering* **2008**, *30* (5), 387–392.  
613 <https://doi.org/10.1080/01919510802336731>.
- 614 (19) Cai, M.; Sun, P.; Zhang, L.; Huang, C.-H. UV/Peracetic Acid for Degradation of  
615 Pharmaceuticals and Reactive Species Evaluation. *Environ. Sci. Technol.* **2017**, *51* (24), 14217–  
616 14224. <https://doi.org/10.1021/acs.est.7b04694>.
- 617 (20) Ao, X.; Eloranta, J.; Huang, C.-H.; Santoro, D.; Sun, W.; Lu, Z.; Li, C. Peracetic Acid-  
618 Based Advanced Oxidation Processes for Decontamination and Disinfection of Water: A  
619 Review. *Water Research* **2021**, *188*, 116479. <https://doi.org/10.1016/j.watres.2020.116479>.
- 620 (21) Nihemaiti, M.; Huynh, N.; Mailler, R.; Mèche-Ananit, P.; Rocher, V.; Barhdadi, R.;  
621 Moilleron, R.; Le Roux, J. High-Resolution Mass Spectrometry Screening of Wastewater  
622 Effluent for Micropollutants and Their Transformation Products during Disinfection with  
623 Performic Acid. *ACS EST Water* **2022**, *2* (7), 1225–1233.  
624 <https://doi.org/10.1021/acsestwater.2c00075>.
- 625 (22) Domínguez-Henao, L.; Turolla, A.; Monticelli, D.; Antonelli, M. Assessment of a  
626 Colorimetric Method for the Measurement of Low Concentrations of Peracetic Acid and

- Hydrogen Peroxide in Water. *Talanta* **2018**, *183*, 209–215.  
<https://doi.org/10.1016/j.talanta.2018.02.078>.
- (23) Hoops, S.; Sahle, S.; Gauges, R.; Lee, C.; Pahle, J.; Simus, N.; Singhal, M.; Xu, L.; Mendes, P.; Kummer, U. COPASI—a COMplex PATHway SIMulator. *Bioinformatics* **2006**, *22* (24), 3067–3074. <https://doi.org/10.1093/bioinformatics/btl485>.
- (24) Von Gunten, U. Ozonation of Drinking Water: Part II. Disinfection and by-Product Formation in Presence of Bromide, Iodide or Chlorine. *Water Research* **2003**, *37* (7), 1469–1487. [https://doi.org/10.1016/S0043-1354\(02\)00458-X](https://doi.org/10.1016/S0043-1354(02)00458-X).
- (25) Le Roux, J.; Gallard, H.; Croué, J.-P. Chloramination of Nitrogenous Contaminants (Pharmaceuticals and Pesticides): NDMA and Halogenated DBPs Formation. *Water Research* **2011**, *45* (10), 3164–3174. <https://doi.org/10.1016/j.watres.2011.03.035>.
- (26) Le Roux, J.; Gallard, H.; Croué, J.-P. Formation of NDMA and Halogenated DBPs by Chloramination of Tertiary Amines: The Influence of Bromide Ion. *Environ. Sci. Technol.* **2012**, *46* (3), 1581–1589. <https://doi.org/10.1021/es203785s>.
- (27) Domínguez Henao, L.; Delli Compagni, R.; Turolla, A.; Antonelli, M. Influence of Inorganic and Organic Compounds on the Decay of Peracetic Acid in Wastewater Disinfection. *Chemical Engineering Journal* **2018**, *337*, 133–142. <https://doi.org/10.1016/j.cej.2017.12.074>.
- (28) Guilloso, R.; Le Roux, J.; Mailler, R.; Vulliet, E.; Morlay, C.; Nauleau, F.; Gasperi, J.; Rocher, V. Organic Micropollutants in a Large Wastewater Treatment Plant: What Are the Benefits of an Advanced Treatment by Activated Carbon Adsorption in Comparison to Conventional Treatment? *Chemosphere* **2019**, *218*, 1050–1060. <https://doi.org/10.1016/j.chemosphere.2018.11.182>.
- (29) Huynh, N.; Caupos, E.; Peirera, C.; Le Roux, J.; Bressy, A.; Moilleron, R. Evaluation of Sample Preparation Methods for Non-Target Screening of Organic Micropollutants in Urban Waters Using High-Resolution Mass Spectrometry. *Molecules* **2021**, *26*, 7064. <https://doi.org/10.3390/molecules26237064>.
- (30) Yuan, Z.; Ni, Y.; Van Heiningen, A. R. P. Kinetics of Peracetic Acid Decomposition: Part I: Spontaneous Decomposition at Typical Pulp Bleaching Conditions. *Can. J. Chem. Eng.* **1997**, *75* (1), 37–41. <https://doi.org/10.1002/cjce.5450750108>.
- (31) Yuan, Z.; Ni, Y.; Van Heiningen, A. R. P. Kinetics of the Peracetic Acid Decomposition: Part II: PH Effect and Alkaline Hydrolysis. *Can. J. Chem. Eng.* **1997**, *75* (1), 42–47. <https://doi.org/10.1002/cjce.5450750109>.
- (32) Sun, X.; Zhao, X.; Du, W.; Liu, D. Kinetics of Formic Acid-Autocatalyzed Preparation of Performic Acid in Aqueous Phase. *Chinese Journal of Chemical Engineering* **2011**, *19* (6), 964–971. [https://doi.org/10.1016/S1004-9541\(11\)60078-5](https://doi.org/10.1016/S1004-9541(11)60078-5).
- (33) Leveneur, S.; Thönes, M.; Hébert, J.-P.; Taouk, B.; Salmi, T. From Kinetic Study to Thermal Safety Assessment: Application to Peroxyformic Acid Synthesis. *Ind. Eng. Chem. Res.* **2012**, *51* (43), 13999–14007. <https://doi.org/10.1021/ie3017847>.
- (34) Everett, A. J.; Minkoff, G. J. The Dissociation Constants of Some Alkyl and Acyl Hydroperoxides. *Trans. Faraday Soc.* **1953**, *49*, 410. <https://doi.org/10.1039/tf9534900410>.

- 667 (35) Koubek, E.; Haggett, M. L.; Battaglia, C. J.; Ibne-Rasa, K. M.; Pyun, H. Y.; Edwards,  
668 J. O. Kinetics and Mechanism of the Spontaneous Decompositions of Some Peroxoacids,  
669 Hydrogen Peroxide and *t*-Butyl Hydroperoxide. *J. Am. Chem. Soc.* **1963**, *85* (15), 2263–  
670 2268. <https://doi.org/10.1021/ja00898a016>.
- 671 (36) da Silva, W. P.; Carlos, T. D.; Cavallini, G. S.; Pereira, D. H. Peracetic Acid: Structural  
672 Elucidation for Applications in Wastewater Treatment. *Water Research* **2020**, *168*, 115143.  
673 <https://doi.org/10.1016/j.watres.2019.115143>.
- 674 (37) Swern, Daniel. Organic Peracids. *Chem. Rev.* **1949**, *45* (1), 1–68.  
675 <https://doi.org/10.1021/cr60140a001>.
- 676 (38) Du, P.; Liu, W.; Cao, H.; Zhao, H.; Huang, C.-H. Oxidation of Amino Acids by  
677 Peracetic Acid: Reaction Kinetics, Pathways and Theoretical Calculations. *Water Research X*  
678 **2018**, *1*, 100002. <https://doi.org/10.1016/j.wroa.2018.09.002>.
- 679 (39) Wang, J.; Chen, W.; Wang, T.; Reid, E.; Krall, C.; Kim, J.; Zhang, T.; Xie, X.; Huang,  
680 C.-H. Bacteria and Virus Inactivation: Relative Efficacy and Mechanisms of Peroxyacids and  
681 Chlor(Am)Ine. *Environ. Sci. Technol.* **2023**, [acs.est.2c09824](https://doi.org/10.1021/acs.est.2c09824).  
682 <https://doi.org/10.1021/acs.est.2c09824>.
- 683 (40) Kato, T.; Uaciquete, D. L. E.; Onodera, G.; Okawa, H.; Sugawara, K.;  
684 Worasuwannarak, N. Changes in the Sulfur Forms of Subbituminous Coals during Oxidation  
685 with Hydrogen Peroxide and Peracetic Acid. *Fuel* **2022**, *330*, 125544.  
686 <https://doi.org/10.1016/j.fuel.2022.125544>.
- 687 (41) Kim, J.; Huang, C.-H. Reactivity of Peracetic Acid with Organic Compounds: A Critical  
688 Review. *ACS EST Water* **2021**, *1* (1), 15–33. <https://doi.org/10.1021/acsestwater.0c00029>.
- 689 (42) von Sonntag, C.; von Gunten, U. *Chemistry of Ozone in Water and Wastewater*  
690 *Treatment*; IWA Publishing, 2012; 312p, ISBN 978-1-78040-083-9.  
691 <https://doi.org/10.2166/9781780400839>
- 692 (43) Zhang, K.; Zhou, X.; Du, P.; Zhang, T.; Cai, M.; Sun, P.; Huang, C.-H. Oxidation of  $\beta$ -  
693 Lactam Antibiotics by Peracetic Acid: Reaction Kinetics, Product and Pathway Evaluation.  
694 *Water Research* **2017**, *123*, 153–161. <https://doi.org/10.1016/j.watres.2017.06.057>.
- 695 (44) Liu, X.; Yang, Z.; Zhu, W.; Yang, Y.; Li, H. Prediction of Pharmaceutical and Personal  
696 Care Products Elimination during Heterogeneous Catalytic Ozonation via Chemical Kinetic  
697 Model. *Journal of Environmental Management* **2022**, *319*, 115662.  
698 <https://doi.org/10.1016/j.jenvman.2022.115662>.
- 699 (45) Lee, Y.; Kovalova, L.; McArdell, C. S.; von Gunten, U. Prediction of Micropollutant  
700 Elimination during Ozonation of a Hospital Wastewater Effluent. *Water Research* **2014**, *64*,  
701 134–148. <https://doi.org/10.1016/j.watres.2014.06.027>.
- 702 (46) Altmann, J.; Ruhl, A. S.; Zietzschmann, F.; Jekel, M. Direct Comparison of Ozonation  
703 and Adsorption onto Powdered Activated Carbon for Micropollutant Removal in Advanced  
704 Wastewater Treatment. *Water Research* **2014**, *55*, 185–193.  
705 <https://doi.org/10.1016/j.watres.2014.02.025>.
- 706 (47) Emmons, W. D. The Oxidation of Amines with Peracetic Acid. *J. Am. Chem. Soc.* **1957**,  
707 *79* (20), 5528–5530. <https://doi.org/10.1021/ja01577a053>.



- (48) Christophoridis, C.; Nika, M.-C.; Aalizadeh, R.; Thomaidis, N. S. Ozonation of Ranitidine: Effect of Experimental Parameters and Identification of Transformation Products. *Sci Total Environ* **2016**, 557–558, 170–182. <https://doi.org/10.1016/j.scitotenv.2016.03.026>.
- (49) Gulde, R.; Clerc, B.; Rutsch, M.; Helbing, J.; Salhi, E.; McArdell, C. S.; von Gunten, U. Oxidation of 51 Micropollutants during Drinking Water Ozonation: Formation of Transformation Products and Their Fate during Biological Post-Filtration. *Water Research* **2021**, 207, 117812. <https://doi.org/10.1016/j.watres.2021.117812>.
- (50) Laurencé, C.; Rivard, M.; Lachaise, I.; Bensemhoun, J.; Martens, T. Preparative Access to Transformation Products (TPs) of Furosemide: A Versatile Application of Anodic Oxidation. *Tetrahedron* **2011**, 67 (49), 9518–9521. <https://doi.org/10.1016/j.tet.2011.10.006>.
- (51) Laurencé, C.; Rivard, M.; Martens, T.; Morin, C.; Buisson, D.; Bourcier, S.; Sablier, M.; Oturan, M. A. Anticipating the Fate and Impact of Organic Environmental Contaminants: A New Approach Applied to the Pharmaceutical Furosemide. *Chemosphere* **2014**, 113, 193–199. <https://doi.org/10.1016/j.chemosphere.2014.05.036>.
- (52) Bourgin, M.; Beck, B.; Boehler, M.; Borowska, E.; Fleiner, J.; Salhi, E.; Teichler, R.; von Gunten, U.; Siegrist, H.; McArdell, C. S. Evaluation of a Full-Scale Wastewater Treatment Plant Upgraded with Ozonation and Biological Post-Treatments: Abatement of Micropollutants, Formation of Transformation Products and Oxidation by-Products. *Water Research* **2018**, 129, 486–498. <https://doi.org/10.1016/j.watres.2017.10.036>.
- (53) Zou, J.; Chen, Q.; Tang, S.; Jin, X.; Chen, K.; Zhang, T.; Xiao, X. Olaquinox-Induced Genotoxicity and Oxidative DNA Damage in Human Hepatoma G2 (HepG2) Cells. *Mutation Research/Genetic Toxicology and Environmental Mutagenesis* **2009**, 676 (1–2), 27–33. <https://doi.org/10.1016/j.mrgentox.2009.03.001>.
- (54) Chen, Y.; Zhang, H. Complexation Facilitated Reduction of Aromatic *N*-Oxides by Aqueous Fe<sup>II</sup>–Tiron Complex: Reaction Kinetics and Mechanisms. *Environ. Sci. Technol.* **2013**, 47 (19), 11023–11031. <https://doi.org/10.1021/es402655a>.

## TOC Graphic

